AD-A164 706 MIXED-ORDER FINITE ELEMENTS FOR THE SOLUTION OF THREE-DIMENSIONAL ELECTRO..(U) CARNEGIE-MELLON UNIV PITTSBURGH PA DEPT OF ELECTRICAL AND COM.. 1/1

UNCLASSIFIED Z J CENDES ET AL. JAN 86 RADC-TR-85-158 F/G 20/4 NL

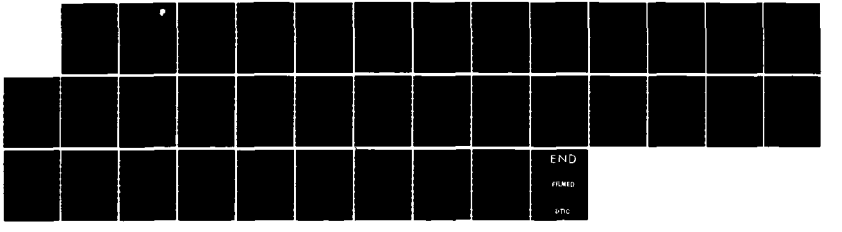

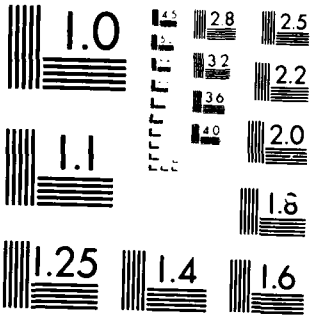

(12)

AD-A164 786

RADC-TR-85-158
Interim Report
January 1986

MIXED-ORDER FINITE ELEMENTS FOR THE SOLUTION OF THREE-DIMENSIONAL ELECTROMAGNETIC FIELDS

Carnegie-Mellon University

Z. J. Cendes
D. Hudak
D. Sun

APPROVED FOR PUBLIC RELEASE; DISTRIBUTION UNLIMITED

ROME AIR DEVELOPMENT CENTER
Air Force Systems Command
Griffiss Air Force Base, NY 13441-5700

This report has been reviewed by the RADC Public Affairs Office (PA) and is releasable to the National Technical Information Service (NTIS). At NTIS it will be releasable to the general public, including foreign nations.

RADC-TR-85-158 has been reviewed and is approved for publication.

APPROVED: Robert McGahan

ROBERT V. McGAHAN
Project Engineer

APPROVED: Allan C. Schell

ALLAN C. SCHELL
Chief, Electromagnetic Sciences Division

FOR THE COMMANDER: John A. Ritz

JOHN A. RITZ
Plans & Programs Office

If your address has changed or if you wish to be removed from the RADC mailing list, or if the addressee is no longer employed by your organization, please notify RADC (EECT), Hanscom AFB MA 01731. This will assist us in maintaining a current mailing list.

Do not return copies of this report unless contractual obligations or notices on a specific document requires that it be returned.

UNCLASSIFIED
SECURITY CLASSIFICATION OF THIS PAGE

AD-A174 936

REPORT DOCUMENTATION PAGE

1a REPORT SECURITY CLASSIFICATION UNCLASSIFIED	1b RESTRICTIVE MARKINGS N/A
2a SECURITY CLASSIFICATION AUTHORITY N/A	3 DISTRIBUTION / AVAILABILITY OF REPORT Approved for public release; distribution unlimited
2b DECLASSIFICATION / DOWNGRADING SCHEDULE N/A	
4 PERFORMING ORGANIZATION REPORT NUMBER(S) N/A	5 MONITORING ORGANIZATION REPORT NUMBER(S) RADC-TR-85-158
6a NAME OF PERFORMING ORGANIZATION Carnegie-Mellon University 6b OFFICE SYMBOL (If applicable)	7a NAME OF MONITORING ORGANIZATION Rome Air Development Center (EECT)
6c ADDRESS (City, State, and ZIP Code) Pittsburgh PA 15213	7b ADDRESS (City, State, and ZIP Code) Hanscom AFB MA 01731
8a NAME OF FUNDING / SPONSORING ORGANIZATION Rome Air Development Center 8b OFFICE SYMBOL (If applicable) EECT	9 PROCUREMENT INSTRUMENT IDENTIFICATION NUMBER F19628-83-C-0079
8c ADDRESS (City, State, and ZIP Code) Hanscom AFB MA 01731	10 SOURCE OF FUNDING NUMBERS PROGRAM ELEMENT NO: 61102F; PROJECT NO: 2305; TASK NO: J4; WORK UNIT ACCESSION NO: 52

11 TITLE (Include Security Classification)
MIXED -ORDER FINITE ELEMENTS FOR THE SOLUTION OF THREE-DIMENSIONAL ELECTROMAGNETIC FIELDS

12 PERSONAL AUTHOR(S)
Z.J. Cendes, D. Hudak, D. Sun

13a TYPE OF REPORT	13b TIME COVERED	14 DATE OF REPORT (Year, Month, Day)	15 PAGE COUNT
Interim	FROM Sep 83 TO Sep 84	January 1986	38

16 SUPPLEMENTARY NOTATION
N/A

17 COSATI CODES		
FIELD	GROUP	SUB-GROUP
17	09	
20	03, 14	

18 SUBJECT TERMS (Continue on reverse if necessary and identify by block number)
Bistatic scattering, Cloning, Finite elements, Measurements

19 ABSTRACT (Continue on reverse if necessary and identify by block number)

A new method for modeling electromagnetic waves by the finite element method is presented. The method is based on a numerical formulation in which different orders of polynomials are used to approximate the three different components of either the electric or the magnetic field vectors. It provides a reliable procedure for the finite element solution of three-dimensional electromagnetic field problems. Heretofore, such solutions were plagued by the presence of spurious modes. The new method is applied to the analysis of fields in resonant electromagnetic cavities.

20 DISTRIBUTION / AVAILABILITY OF ABSTRACT	21 ABSTRACT SECURITY CLASSIFICATION
☐ UNCLASSIFIED/UNLIMITED ☒ SAME AS RPT ☐ DTIC USERS	UNCLASSIFIED
22a NAME OF RESPONSIBLE INDIVIDUAL Robert V. McGahan	22b TELEPHONE (Include Area Code) (617) 861-2050
	22c OFFICE SYMBOL RADC (EECT)

DD FORM 1473, 84 MAR 83 APR edition may be used until exhausted. All other editions are obsolete.

SECURITY CLASSIFICATION OF THIS PAGE
UNCLASSIFIED

Mixed-Order Finite Elements for the Solution of Three-Dimensional Electromagnetic Fields

Z.J. Cendes, D. Hudak, D. Sun

Electrical & Computer Engineering
Carnegie-Mellon University
Pittsburgh, PA 15213

Abstract

A new method for modeling electromagnetic waves by the finite element method is presented. The method is based on a numerical formulation in which different orders of polynomials are used to approximate the three different components of either the electric or the magnetic field vectors. It provides a reliable procedure for the finite element solution of three-dimensional electromagnetic field problems. Heretofore, such solutions were plagued by the presence of spurious modes. The new method is applied to the analysis of fields in resonant electromagnetic cavities.

Introduction

The finite element method is often advanced as a useful numerical procedure for modeling high-frequency electromagnetic wave phenomena. Applied at an early date to solve homogeneous waveguide problems,[1] the method proved to be extremely accurate and reliable for these problems. However, when the method was applied to the study of inhomogeneous waveguides and to the solution of three-dimensional resonant cavity and scattering problems, difficulties in the form of "spurious" modes were encountered. Spurious modes are non-physical solutions of the electromagnetic field equations that are computed simultaneously with the correct physical solutions.

Since the presence of spurious modes in a numerical solution can destroy the validity of the solution, much effort has been directed at reducing or eliminating the unwanted modes. The first approach, originally suggested by Konrad[2], is to enforce the electromagnetic field boundary conditions exactly on the finite element approximation space. This procedure has been used by Mabaya, Lagasse and Vandenbulke[3] in the E_z - H_z formulation and by Davies, Fernandez and Philippon[4] and by Rahman and Davies[5] in the 3-component H formulation; all three papers report only limited success in eliminating spurious modes by this technique. Recently, Koshiba, Hayata, and Suzuki[6] have shown that rigorous enforcement of boundary conditions does indeed eliminate spurious modes above the "air line" (i.e. the line $\beta/k_o = 1$ in a β/k_o versus k_o plot) but does not work in general below the air line.

The second approach to eliminating spurious modes is to modify the variational principle used to approximate the fields. Working independently, Winkler and Davies[7] and Hara, Wada, Fukasawa and Kikuchi[8] have recognized that the spurious modes do not satisfy the zero divergence condition on the

A-1

electric or magnetic field. Both references suggest adding a penalty term proportional to the norm of the divergence of the field to the governing variational principle. Unfortunately, this procedure does not eliminate the spurious modes completely. However, as demonstrated in reference 8, the spurious modes are not stable with respect to the amount of penalty, and can be distinguished from correct solutions by plotting the finite element eigenvalue spectra with respect to the penalty parameter. Of course, this procedure is highly inefficient and cumbersome: each new field problem must be solved repeatedly and all of the eigenvalues plotted in order to identify the correct ones.

A different but related procedure to reduce the number of spurious modes was proposed recently by Konrad.[9] References 7 and 8 are based on minimizing a functional derived from the vector wave equation with the addition of a zero-divergence penalty term. Konrad suggests using the vector Helmholtz equation instead and finds that "... a great number, though not all of the spurious solutions are indeed eliminated." This result is not surprising since the variational expressions derived for the vector Helmholtz equation and for the vector wave equation with the addition of a unit penalty term are identical in the case of homogeneous media.

The third approach to eliminating spurious modes in finite element solutions is to restrict the finite element approximation functions to lie in a reduced function space. In this view, spurious modes are the result of using improper functions in the variational procedure. To ensure that only correct solutions are generated, one must employ only admissible functions in the finite element approximation. *This is the* approach taken in this report.

The use of a restricted function space to eliminate spurious modes in finite element analysis was first suggested by Hano.[10] Hano showed that, in two dimensional problems, spurious modes are completely eliminated by using combination constant-linear finite element approximation functions. These functions have two interesting properties: (1) their divergence is identically zero, and (2) they are discontinuous at element boundaries.

In this report, we derive a set of restricted finite element basis functions for the solution of three dimensional electromagnetic field problems and show that only correct, physical solutions are obtained with the new functions. As in the case in reference 10, the functions reported here employ different orders of polynomial approximation in different directions in each element. However, in our case, the approximation functions are continuous across element boundaries and are not restricted to be non-divergent.

Formulation of the EM Field Equations

Electromagnetic wave propagation is governed by the vector wave equations

$$\nabla \times \frac{1}{\mu_r} \nabla \times \mathbf{E} = \epsilon_r k_o^2 \mathbf{E} \tag{1}$$

$$\nabla \times \frac{1}{\epsilon_r} \nabla \times \mathbf{H} = \mu_r k_o^2 \mathbf{H} \tag{2}$$

where μ_r and ϵ_r are the relative permeability and relative permittivity of the material, respectively, and $k_o^2 = \omega^2 \mu_o \epsilon_o$. At the interface between two dielectrics, the tangential components of the electric and magnetic fields must be continuous

$$\mathbf{1}_n \times (\mathbf{E}^{(1)} - \mathbf{E}^{(2)}) = 0 \tag{3}$$

$$\mathbf{1}_n \times (\mathbf{H}^{(1)} - \mathbf{H}^{(2)}) = 0 \tag{4}$$

while the normal components are discontinuous as follows

$$\mathbf{1}_n \bullet (\epsilon_1 \mathbf{E}^{(1)} - \epsilon_2 \mathbf{E}^{(2)}) = 0 \tag{5}$$

$$\mathbf{1}_n \bullet (\mu_1 \mathbf{H}^{(1)} - \mu_2 \mathbf{H}^{(2)}) = 0 \tag{6}$$

In these equations, superscripts (1) and (2) refer to media 1 and media 2, respectively.

In the remainder of this report, we shall use the electric field **E** as the unknown. Obviously, a similar treatment holds for **H**. In terms of **E**, equation (4) becomes

$$\mathbf{1}_n \times (\frac{1}{\mu_1} \nabla \times \mathbf{E}^{(1)} - \frac{1}{\mu_2} \nabla \times \mathbf{E}^{(2)}) = 0 \tag{7}$$

We must therefore solve equation (1) subject to the interface conditions (3), (5) and (7).

Konrad[1] has shown that the Euler equation of the functional

$$F = \frac{1}{2} \int \{\frac{1}{\mu_r} |\nabla \times \mathbf{E}|^2 - \epsilon_r k_o^2 |\mathbf{E}|^2\} d\Omega \tag{8}$$

is equation (1) and that the corresponding natural boundary equation (7) is the natural boundary condition for this functional. One may therefore approximate the electric field **E** by expanding **E** in terms of basis functions, apply the essential boundary conditions (3) and (5) explicitly, and minimize F to obtain **E**.

While the solution process described above has been widely reported in the literature[2,4-7,10-13], as noted in the introduction, there are serious problems. To eliminate these problems, we need to define the approximation functions for **E** more carefully.

A Basis for Curl

To solve for **E** via equation (8), we must find a legitimate approximation for the curl operator. The operator curl has a domain, a nullspace and a range; it is not enough – as had been done in the past – to approximate only the domain.

The nullspace of an operator is defined to be the set of functions that produce zero when the operator acts on it

$$N(A) = \{x: \quad Ax = 0 \qquad for\ all\ x\} \tag{9}$$

It is well known that the nullspace of the curl operator is provided by the gradient operator

$$N(curl) = \nabla \phi \tag{10}$$

where ϕ is an arbitrary scalar.

Let us approximate ϕ by finite basis functions $\tilde{\alpha}(x,y,z)$ over a rectangular parallelepiped. These basis functions are defined in Appendix A and result in the expression

$$\phi(x,y,z) = \tilde{\alpha}^{(m,n,p)}(x,y,z)\underset{\sim}{\phi} \tag{11}$$

The polynomial $\tilde{\alpha}^{(m,n,p)}(x,y,z)$ is m'th order in the x-direction, n'th order in y, and p'th order in z. Since the derivative of an n'th order polynomial is (n-1)'st order, it follows that the nullvectors of the curl operator must have the form

$$\begin{aligned} E_x(x,y,z) &= \tilde{\alpha}^{(m-1,n,p)}\underset{\sim}{E}_x \\ E_y(x,y,z) &= \tilde{\alpha}^{(m,n-1,p)}\underset{\sim}{E}_y \\ E_z(x,y,z) &= \tilde{\alpha}^{(m,n,p-1)}\underset{\sim}{E}_z \end{aligned} \tag{12}$$

We may write this in the compact form

$$\mathbf{E} = \gamma\underset{\sim}{\mathbf{E}} \tag{13}$$

where

$$\gamma = \begin{bmatrix} \tilde{\alpha}^{(m-1,n,p)} & 0 & 0 \\ 0 & \tilde{\alpha}^{(m,n-1,p)} & 0 \\ 0 & 0 & \tilde{\alpha}^{(m,n,p-1)} \end{bmatrix} \tag{14}$$

$$\underset{\sim}{\mathbf{E}} = \begin{bmatrix} \underset{\sim}{\mathbf{E}}_x \\ \underset{\sim}{\mathbf{E}}_y \\ \underset{\sim}{\mathbf{E}}_z \end{bmatrix} \tag{15}$$

The curl of **E** is evaluated as

$$\nabla \times \mathbf{E} = \begin{bmatrix} 0 & -\partial/\partial z & \partial/\partial y & E_x \\ \partial/\partial z & 0 & -\partial/\partial x & E_y \\ -\partial/\partial y & \partial/\partial x & 0 & E_z \end{bmatrix} \tag{16}$$

Substituting (13) into (16) gives

$$\nabla \times \mathbf{E} = \beta \mathbf{C} \underset{\sim}{\mathbf{E}} \tag{17}$$

where

$$\beta = \begin{bmatrix} \underset{\sim}{\alpha}^{(m,n-1,p-1)} & 0 & 0 \\ 0 & \underset{\sim}{\alpha}^{(m-1,n,p-1)} & 0 \\ 0 & 0 & \underset{\sim}{\alpha}^{(m-1,n-1,p)} \end{bmatrix} \tag{18}$$

$$\mathbf{C} = \begin{bmatrix} 0 & -D_z & D_y \\ D_z & 0 & -D_x \\ -D_y & D_x & 0 \end{bmatrix}$$

where the matrices D_i are called differentiation matrices and are defined in Appendix 2.

We note that the factorization in equation (17) is not possible if the same order of polynomial is used to approximate E_i in all three directions.

The basis functions in equations (11), (13), and (17) provide a consistent representation of the nullspace, domain, and range of the curl operator, respectively. The dimension of the nullspace is equal to the number of parameters in $\underset{\sim}{\phi}$; this is

$$Dim(N(curl)) = (m+1)(n+1)(p+1) \tag{19}$$

The dimensions of the domain and range spaces are equal to the number of independent basis functions in γ and β; these are

$$Dim\ (D(curl)) = 3mnp + 2mn + 2mp + 2np + m + n + p \tag{20}$$

$$Dim\ (R(curl)) = 3mnp + np + mp + mn \tag{21}$$

The rank of the matrix **C** is equal to the dimension of the domain space minus the dimension of the nullspace

$$Rank(\mathbf{C}) = 2mnp + mn + mp + np - 1 \tag{22}$$

Computing the Matrix Elements

Substituting equations (13) and (17) into equation (8) and minimizing with respect to the coefficients $\underset{\sim}{E}$ results in the matrix equation

$$\mathbf{C}^T\mathbf{K}\mathbf{C}\ \underset{\sim}{E} = k_o^2\mathbf{M}\ \underset{\sim}{E} \tag{23}$$

where **K** and **M** are the matrices

$$\mathbf{K} = \int \frac{1}{\mu_r}\beta^T\beta\ d\Omega \tag{24}$$

$$\mathbf{M} = \int \epsilon_r\gamma^T\gamma\ d\Omega \tag{25}$$

To evaluate the matrix elements in **K** and **M**, it is sufficient to evaluate the integral

$$\mathbf{G}^{(r,s,t)} = \int \tilde{\alpha}^{T(r,s,t)}\tilde{\alpha}^{(r,s,t)}d\Omega \tag{26}$$

Substituting equation (A13) into (26) gives

$$\mathbf{G} = (1/L_xL_yL_z)\int(\tilde{\alpha}^r(\varsigma)\otimes\tilde{\alpha}^s(\xi)\otimes\tilde{\alpha}^t(\lambda))^T\ (\tilde{\alpha}^r(\varsigma)\otimes\tilde{\alpha}^s(\xi)\otimes\tilde{\alpha}^t(\lambda))d\varsigma d\xi d\lambda) \tag{27}$$

Introducing Kroneckers identities (iii) and (v) converts this into

$$\mathbf{G} = (1/L_xL_yL_z)T^{(r)}\otimes T^{(s)}\otimes T^{(t)} \tag{28}$$

where

$$T^{(i)} = \int\tilde{\alpha}^{(i)T}(\varsigma)\ \tilde{\alpha}^{(i)}(\varsigma)d\varsigma \tag{29}$$

Thus, only the one dimensional T matrix is required to evaluate G. Numerical values of the first two T matrics are

$$\mathbf{T}^{(1)} = \frac{1}{6}\begin{bmatrix} 2 & 1 \\ 1 & 2 \end{bmatrix} \tag{30}$$

$$\mathbf{T}^{(2)} = \frac{1}{30}\begin{bmatrix} 4 & 2 & -1 \\ 2 & 16 & 2 \\ -1 & 2 & 4 \end{bmatrix} \tag{31}$$

To evaluate the finite element coefficient matrix for one element, one therefore needs to form the matrices **K** and **M** using equations (28) and (29), evaluate **C** by using the values in Appendix B, and pre-

and post-multiply $\mathbf{K}$ by $\mathbf{C}^T$ and $\mathbf{C}$, respectively. The contribution from each element is combined with the other elements in the grid to form a large, sparse matrix eigenvalue problem. This eigenvalue problem is solved by using established techniques for the eigenvalues k_0^2 and eigenvectors $\underset{\sim}{E}$.

Computational Results

A computer program has been developed based on the above formulation to solve for the electromagnetic fields in resonant cavities. The program allows finite elements of mixed orders to be assembled and solved for complex three-dimensional geometries. A significant component of this work was the development of a sparse matrix eigenvalue solution package based on the Lanczos algorithm.

Some of the computational results obtained from the program are presented in Tables 1-12. In these tables, the approximate eigenvalues obtained by the finite element method for rectangular parallelpiped cavities are presented along with the exact analytical values.

To begin, Tables 1 and 2 present the eigenvalue spectrum for the "traditional" finite element solution of the vector wave equation in which each component of the electric field is approximated *in all directions* by a linear polynomial (8-node elements). Spurious nodes are evident in the spectrum, both below the dominant physical node and above it. It is obviously very difficult to distinguish good solutions from bad solutions with this approach.

Now consider the case of constant-bilinear elements ($m = n = p = 1$; 4 node elements). The eigenvalue spectrums for two different cavities obtained by using these elements are presented in Tables 3 and 4. Notice that in this case a one-to-one correspondence exists between the approximate eigenvalues and the exact ones, with the dominant eigenvalue being approximated reasonably well. Although some fairly large errors are obtained with the high-order nodes in Tables 3 and 4, these errors are a result of the small number of elements used in this problem. It is significant that each mode in these solutions can be identified; greater accuracy in the eigenvalues can be obtained when more elements are employed.

For constant-bilinear elements the dimension of the nullspace is $N = 2 \times 2 \times 2 = 8$. Corresponding to this nullity, eight zero eigenvalues are found in Tables 3 and 4. Zero eigenvalues have been computed in this work to confirm theoretical predictions; in practice, one may save computer time by computing the positive eigenvalues only.

Solutions obtained by using linear-biquadratic elements ($m = n = p = 2$; 18 node elements) are presented in Tables 5 and 6. These solutions are seen to be much more precise than the constant bilinear element solutions. The reason for the increased accuracy is twofold: (1) Higher-order polynomials are more accurate than low-order polynomials, and (2) linear-biquadratic elements are continuous across element boundaries while the constant-bilinear elements are not. A vector plot of the field at a height z

= 0.35 above the bottom of the cavity is shown in Figure 1. In the case of linear-biquadratic elements, the nullity of the curl operator is N = 3 x 3 x 3 = 27. This is equal to the number of zero eigenvalues computed for the problems in Tables 5 and 6.

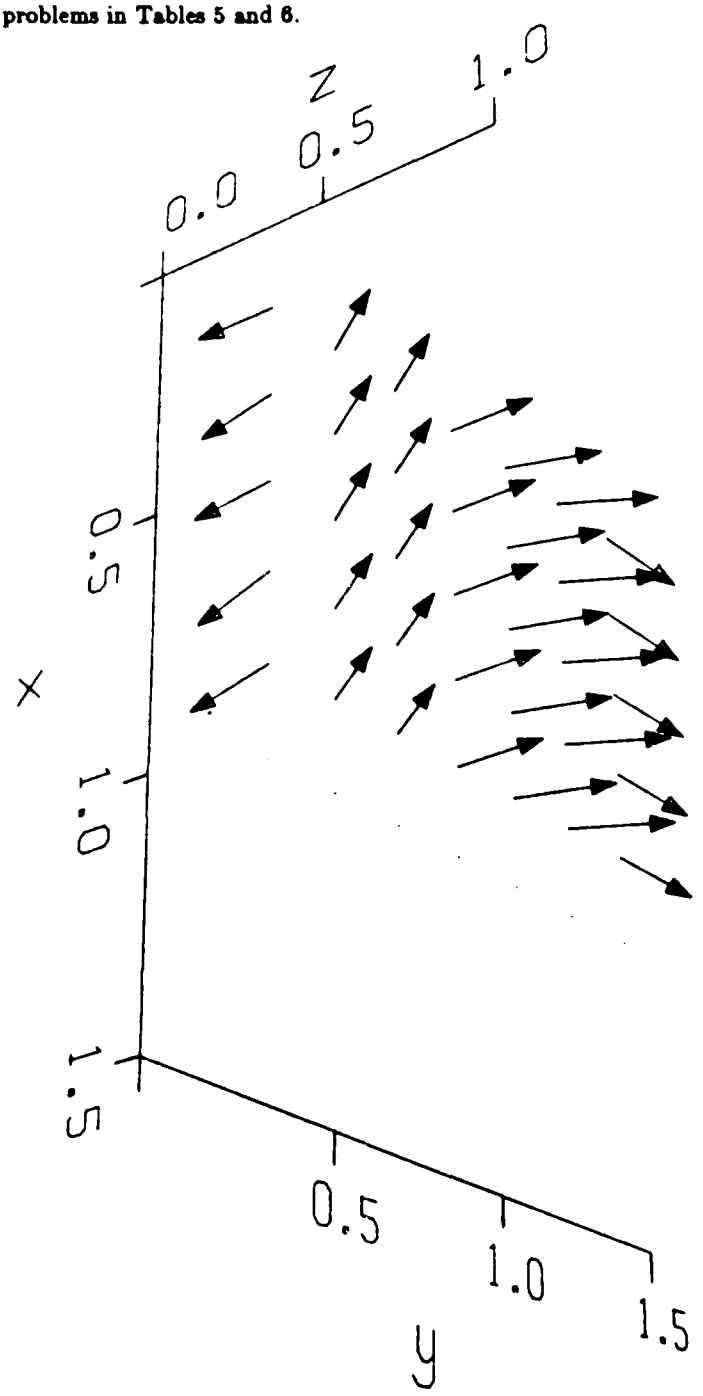

Figure 1: Plot of the electric field for the dominate mode in a cavity of dimensions $\pi/3,\pi/3,\pi/3$ at a height of x = 0.35 above the base

Finally, we report some computations obtained by applying the finite element method to the vector Helmholtz equation. The vector Helmholtz equation is separable in a rectangular coordinate system into

three uncoupled one-dimensional Helmholtz equations. Not surprizingly, the eigenvalues of this one-dimensional equation are correctly computed as shown in Tables 7 and 8. However, if one employs the constant-bilinear 4-node element in this approximation then an incomplete solution is produced. As shown in Tables 9-11, the eigenvalues are correct, but only the zero-mode eigenvalues appear. Thus, solutions obtained by using constant-bilinear elements in the Helmholtz equation do not allow the discontinuities at the element edges observed in the solution of the vector wave equations.

When linear-biquadratic elements are used in the vector Helmholtz equation, solutions in the form reported in Table 12 are observed. In this case, all eigenvalues of the cavity are approximated, but the zero-mode eigenvalues where the solution is a constant in one direction are computed far more accurately than the non zero-mode eigenvalues.

As a final confirmation of the correctness of the procedure reported here, observe from Tables 4 and 7 that the solution of the vector wave equation with constant-bilinear elements and of the vector Helmholtz equation with trilinear elements are identical in all modes to six significant figures. It appears that these two ways of solving rectangular cavity problems are numerically identical. As pointed out earlier, however, the advantage of solving the vector wave equation is that it generalizes to modeling non-rectangular cavaties and to cavities involving dielectric boundaries.

Conclusions

Three-dimensional electromagnetic field problems may be solved by using mixed order finite elements to approximate the vector field. In this approach a consistent numerical approximation is made for the domain, range, and null spaces of the curl operator. Such a consistent approximation in the solution of the vector wave equation eliminates the problem of spurious nodes that had plagued previous solution procedures.

References

1. P. Silvester, "A General High-Order Finite-Element Waveguide Analysis Program," IEEE Trans., Vol. MTT-17, pp. 204-210, April 1969.

2. A. Konrad, "Vector Variational Formulation of electromagnetic Fields In Anisotropic Media", IEEE Trans., Vol. MTT-24, pp. 553-559, September 1976.

3. N. Mabaya, P.E. Lagasse and P. Vandenbulke, "Finite Element Analysis of Optical Waveguides," IEEE Trans., Vol. MTT-29, pp. 600-605, June 1981.

4. J.B. Davies, F.A. Fernandez and G.Y. Philippori, "Finite Element Analysis of All Modes in Cavities with Circular Symmetry," IEEE Trans., Vol. MTT-30, pp. 1975-1980, 1982.

5. B.M.A. Rahman and J.B. Davies, "Finite-Element Analysis of Optical and Microwave Waveguide Problems," IEEE Trans., Vol. MTT-32, pp. 20-28, 1984.

6. M. Koshiba, K. Hayota, and M. Suzuki, "Improved Finite-Element Formulation in Terms of the Magnetic Field Vector for Dielectric Waveguides", IEEE Trans., Vol. MTT-33, pp. 227-233, March 1985.

7. J.R. Winkler and J.B. Davies, "Elimination of Spurious Modes in Finite Element Analysis", J. Computational Physics, Vol. 56, pp. 1-14, 1984.

8. M. Hara, T. Wada, T. Fukasawa, and F. Kikuchi, "Three Dimensional Analysis of RF Electromagnetic Field by the Finite Element Method", IEEE Trans., Vol. MAG-19, pp. 2417-2420, Nov. 1983.

9. A. Konrad, "On the Reduction of the Number of Spurious Modes in the Vectorial Finite Element Solution of Three-Dimensional Cavities and Waveguides", General Electric Company, Technical Information Series, Report No. 84 CRD275, October, 1984.

10. M. Hano, "Finite-Element Analysis of Dielectric-Loaded Waveguides," IEEE Trans., Vol. MTT-32, pp. 1275-1279, 1984.

11. R.L. Ferrari and G.L. Maile, "Three-Dimensional Finite Element Method for Solving Electromagnetic Problems", Electronics Letters, Vol. 14, pp. 467-468, 1978.

12. J.P. Webb, G, L. Maile, and R.L. Ferrari, "Finite Element Solution of Three-Dimensional Electromagnetic Problems," IEE Proc. H, Microwaves, Optics and Antennas, Vol. 130, pp. 153-159, 1983.

13. M. de Pourcq, "Field and Power-Density Calculations by Three-Dimensional Finite Elements", IEE Proc. H, Vol. 130, pp. 377-384, 1983.

APPENDIX - A

Rectangular Basis Functions

To see how approximation functions are formed for bricks, first consider the two-dimensional case shown in Figure 1. In this figure, an arbitrary rectangular reference element is mapped into the unit square by the transformation

$$\varsigma = (x - x_R)/L_x \tag{A1}$$

$$\xi = (y - y_R)/L_y \tag{A2}$$

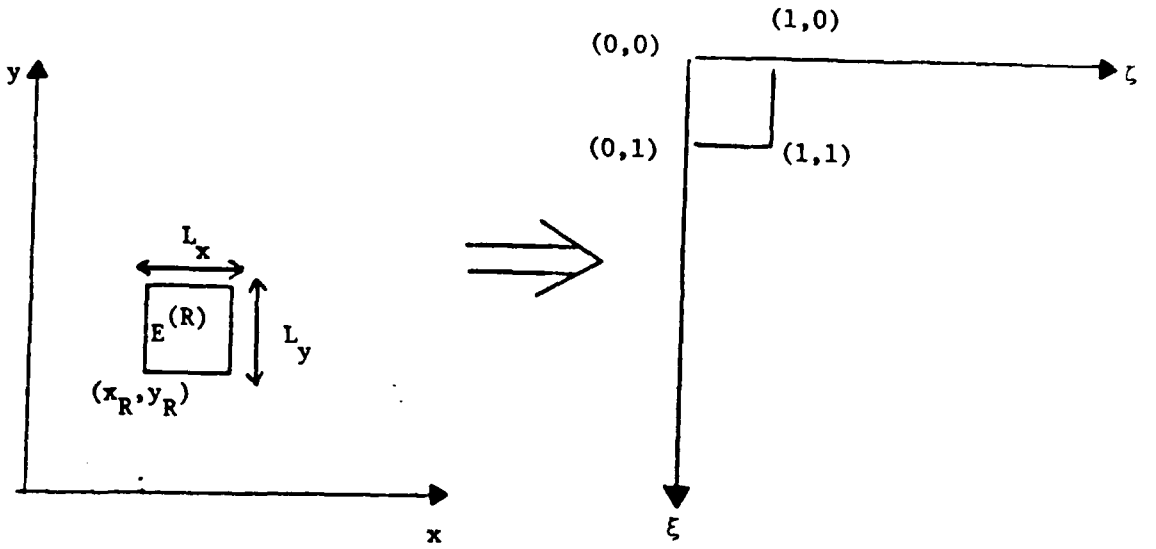

Figure 2: Bilinear mapping of an arbitrary rectangle to the reference rectangle

Two-dimensional basis functions may be obtained from one-dimensional functions by using the Kronecker matrix product.

Definition:

If A is an nxm matrix and B is a pxq matrix, then the Kronecker matrix product of A and B is denoted by $A \otimes B$ and is the npxmq matrix

$$A \otimes B = \begin{matrix} a_{11}B & a_{12}B & \cdots & a_{1m}B \\ \vdots & \vdots & & \vdots \\ a_{n1} & a_{n2}B & \cdots & a_{nm}B \end{matrix} \tag{A3}$$

Kronecker matrix products satisfy the following useful identities[14]

(i) $A \otimes (B+C) = A \otimes B + A \otimes C$

(ii) $\alpha A \otimes \beta B = \alpha\beta (A \otimes B)$

(iii) $AB \otimes CD = (A \otimes C)(B \otimes D)$

(iv) $(A \otimes B)^{-1} = A^{-1} \otimes B^{-1}$

(v) $(A \otimes B)^{T} = A^{T} \otimes B^{T}$

In general, one-dimensional n'th order interpolation polynomials are defined as

$$\alpha^{(n)}_{k}(\varsigma) = \prod_{i=1}^{n+1} \frac{(\varsigma - \varsigma_i)}{(\varsigma_k - \varsigma_i)} \tag{A4}$$

where the ς_i are the interpolation nodes. Using the Kronecker matrix product, two-dimensional interpolation polynomials are given by

$$\tilde{\alpha}^{(n,m)}(\varsigma,\xi) = \tilde{\alpha}^{(n)}(\varsigma) \otimes \tilde{\alpha}^{(m)}(\xi) \tag{A5}$$

For example, the second-order interpolation polynomial $\tilde{\alpha}^{(2,2)}(\varsigma,\xi)$ is the nine element row vector

$$\begin{aligned} \tilde{\alpha}^{(2,2)}(\varsigma,\xi) = [&\alpha_1(\varsigma)\alpha_1(\xi) \;\; \alpha_1(\varsigma)\alpha_2(\xi) \;\; \alpha_1(\varsigma)\alpha_3(\xi) \;\; \alpha_2(\varsigma)\alpha_1(\xi) \\ &\alpha_2(\varsigma)\alpha_2(\xi) \;\; \alpha_2(\varsigma)\alpha_3(\xi) \;\; \alpha_3(\varsigma)\alpha_1(\xi) \;\; \alpha_3(\varsigma)\alpha_2(\varsigma) \;\; \alpha_3(\varsigma)\alpha_3(\xi)] \end{aligned} \tag{A6}$$

The locations of the interpolation nodes of the polynomials $\tilde{\alpha}^{(2,2)}$ are indicated in Figure 2. During computation, the nodes are stored most conveniently by columns; in this case, the axes ς and ξ are oriented as shown in Figure 3.

Now consider approximating an arbitrary function $\phi(\varsigma,\xi)$ in terms of the finite element approximation functions. We may write this as

$$\phi(\varsigma,\xi) = \tilde{\alpha}^{(m)}(\varsigma) \Phi \underset{\sim}{\alpha}^{(n)}(\xi) \tag{A7}$$

where Φ is an m by n matrix of values at the interpolation nodes. Equation (A7) is converted into the standard matrix form

$$\phi(\varsigma,\xi) = \tilde{\alpha}(\varsigma,\xi) \underset{\sim}{\phi} \tag{A8}$$

by defining a vector operation called *vec* in the following manner:

$$\text{VecA} = \begin{bmatrix} \underset{\sim}{A}_1 \\ \underset{\sim}{A}_2 \\ \bullet \\ \bullet \\ \bullet \\ \underset{\sim}{A}_n \end{bmatrix} \tag{A9}$$

where $\underset{\sim}{A}_i$ is the i'th column of the matrix A. The operator vec and the Kronecker product are related by the identity

$$vec\ ABC = (C^{T} \otimes A)\ vecB \tag{A10}$$

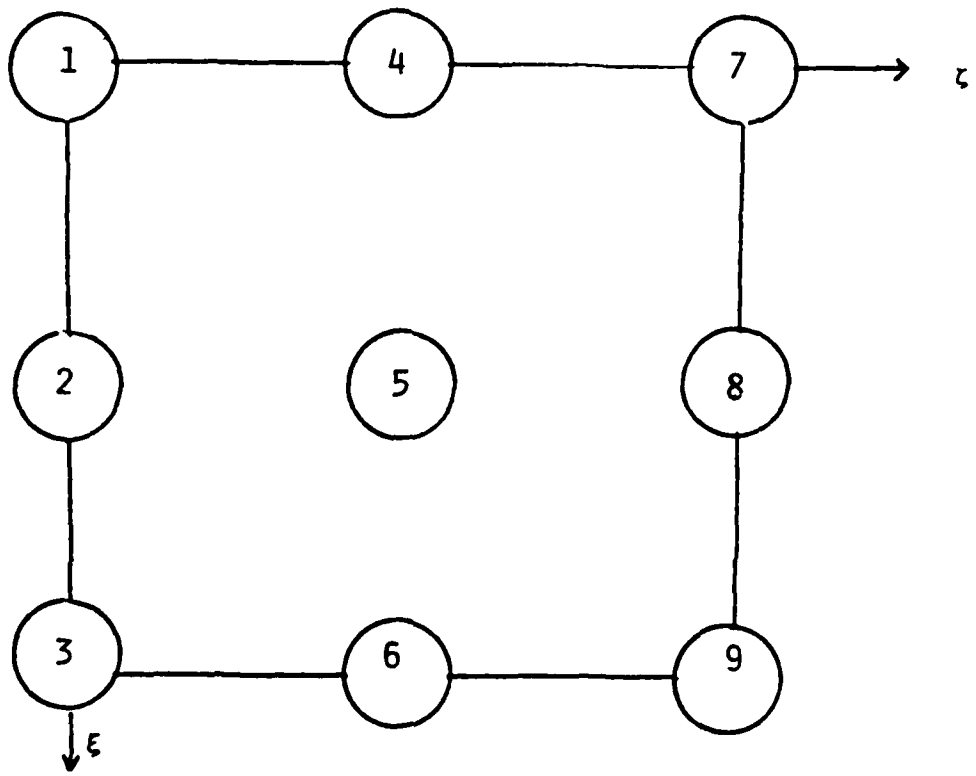

Figure 3: The relative locations of the interpolation nodes corresponding to the polynomial $\alpha^{(2,2)}(\varsigma,\xi)$.

The vec of a scalar is simply itself; therefore, taking vec of both sides of equation (A8) yields

$$\phi(\varsigma,\xi) = (\tilde{\alpha}^{(n)}(\varsigma) \otimes \tilde{\alpha}^{m}(\xi)) \; \underline{\phi} \tag{A11}$$

where

$$\underline{\phi} = vec\Phi \tag{A12}$$

Three-dimensional finite elements are generated by an analogous procedure to that used in two-dimensions. Approximation functions for brick-shaped elements are given by the equation

$$\tilde{\alpha}^{(n,m,p)} = \tilde{\alpha}^{(n)}(\varsigma) \otimes \tilde{\alpha}^{(m)}(\xi) \otimes \alpha^{(p)}(\lambda) \tag{A13}$$

where (ς,ξ,λ) are homogeneous coordinates in the brick. Figure 4 presents the node numbering scheme for the second order case.

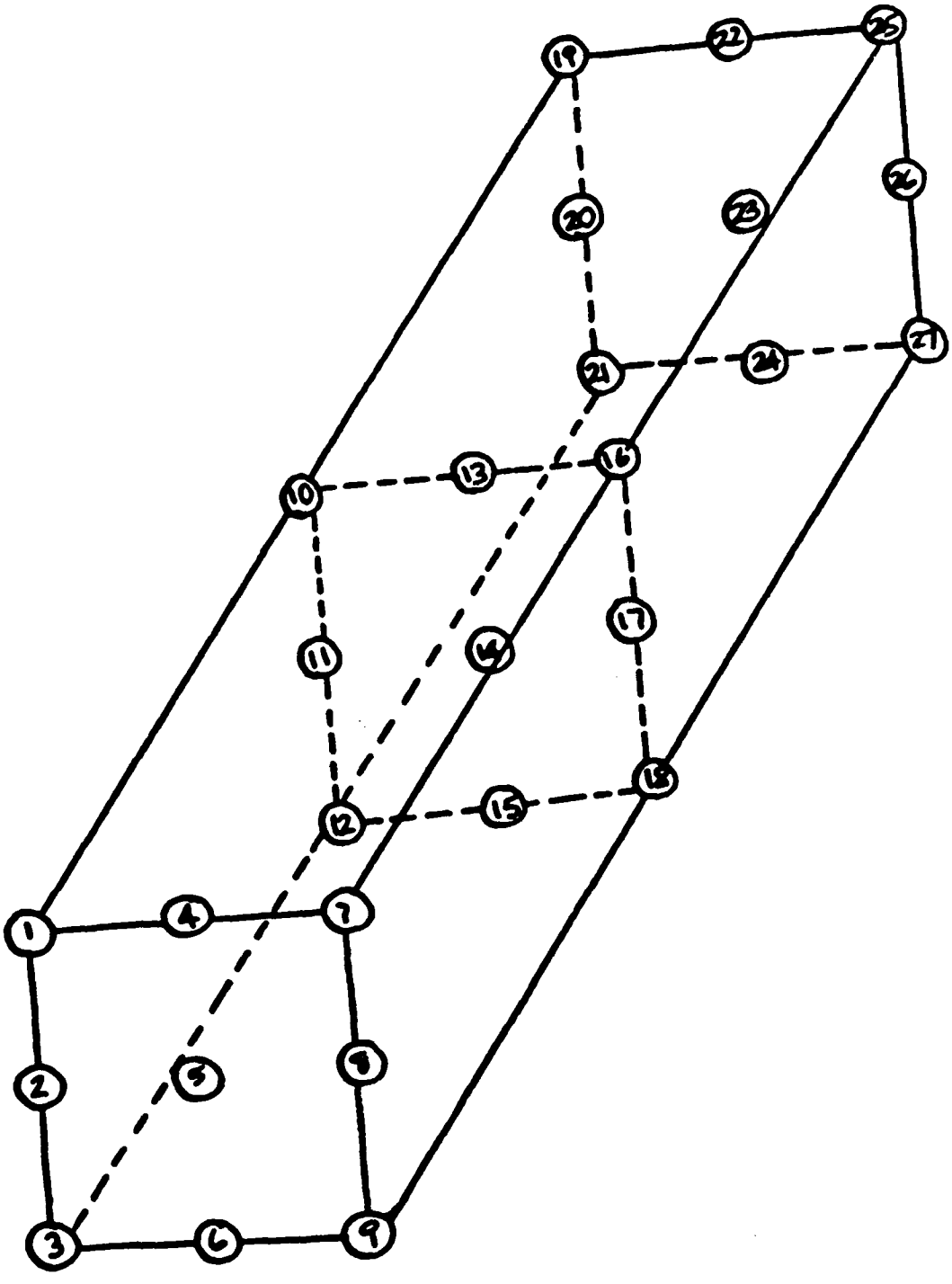

Figure 4: Interpolation node numbering for second order brick elements

APPENDIX - B

Differential Matrices

One-dimensional differentiation matrices are defined by the equation

$$\frac{d\alpha^{(n)}(\varsigma)}{d\varsigma} = \tilde{\alpha}^{(n-1)}(\varsigma)D^{(n)} \tag{B1}$$

where $D^{(n)}$ is the n by n+1 differentiation matrix. The polynomials $\tilde{\alpha}^{(n-1)}(\varsigma)$ in equation (B1) are of one order less than that of $\tilde{\alpha}^{(n)}(\varsigma)$ because the derivative of an n'th order polynomial is (n-1)'st order. Evaluating both sides of equation (B1) at the (n-1)'st order interpolation nodes $a_i^{(n-1)}, i = 1,\ldots,n$ provides the elements of the differentiation matrix as

$$D_{ij}^{(n)} = D_{ij}^{(n)} = \frac{d_j\alpha^{(n)}(\varsigma)}{d\varsigma}\Big|_{\varsigma = a_i^{(n-1)}}$$

Performing the indicated operations with the equispaced node interpolation polynomials gives the numerical values

$$D^{(1)} = \begin{bmatrix} -1. & 1 \end{bmatrix}$$

$$D^{(2)} = \begin{bmatrix} -3 & 4. & -1. \\ 1. & -4. & 3. \end{bmatrix} \tag{B3}$$

$$D^{(3)} = \begin{bmatrix} 05.5 & 9. & -4.5 & 1. \\ .125 & -3.375 & 3.375 & -.125 \\ -1. & 4.5 & -9. & -5.5 \end{bmatrix}$$

Note that the matrix D has the following anti-symmetry property

$$D_{ij}^{(n)} = -D_{n-i+1,n-j+2}^{(n)} \tag{B4}$$

To extend the above result to two-dimensions, we need to evaluate

$$\begin{aligned} \frac{\partial}{\partial\varsigma}\tilde{\alpha}^{(m,n)}(\varsigma,\xi) &= \frac{\partial}{\partial\varsigma}\tilde{\alpha}^{(m)}(\varsigma)\otimes\tilde{\alpha}^{(n)}(\xi) \\ &= \tilde{\alpha}^{(n-1)}(\varsigma)D^{(m)}\otimes\tilde{\alpha}^{(n)}(\xi) \\ &= (\tilde{\alpha}^{(m-1)}(\varsigma)\otimes\tilde{\alpha}^{(n)}(\xi))(D^{(m)}\otimes I) \end{aligned} \tag{B5}$$

Thus we find that

$$\frac{\partial}{\partial\varsigma}\tilde{\alpha}^{(m,n)}(\varsigma,\xi) = \tilde{\alpha}^{(m-1,n)}(\varsigma,\xi)D_\varsigma$$

(B6)

where

$$D_\varsigma = D^{(m)} \otimes I \tag{B7}$$

Similar results hold for derivatives in the ξ-direction and for three-dimensional elements.

List of Figures

CURL-CURL-trilinear functions(8-node elements)

Lx=Ly=Lz=pi/3. (pi=3.1415926535)
number of nodes in x-direction = 12
" y-direction = 12
" z-direction = 12
hx=hy=hz=pi/9.

approx-eigenvalue	modes	actual-eigenvalue
1.96968	-------	--------
9.08752	-------	--------
9.08752		
9.08752		
19.69684	(0,1,1)	18.00000
19.69684		
19.69684	(1,0,1)	
19.69684		
19.69684	(1,1,0)	
19.69684		
28.25468	-------	--------
28.25468		
28.25468		
28.56042	-------	--------
28.56042		
49.24210	-------	--------
59.09051	(0,1,2)	45.00000
59.09051		
59.09051	(0,2,1)	
59.09051		
59.09051	(1,0,2)	
59.09051		
59.09051	(2,0,1)	
59.09051		
59.09051	(1,2,0)	
59.09051		
59.09051	(2,1,0)	
59.09051		
60.83625	-------	--------
60.83625		
60.83625		
67.95409	-------	--------
67.95409		
67.95409		
83.71156	-------	--------
83.71156		
83.71156		
98.48419	(0,2,2)	72.00000
98.48419		
98.48419	(2,0,2)	
98.48419		
98.48419	(2,2,0)	
98.48419		

Table 1. Eigenvalues of the vector wave equation (curl-curl operator) in a rectangular cavity obtained by using trilinear approximation functions. Note that many of the approximate eigenvalues computed do not correspond to any actual physical mode.

CURL-CURL-trilinear functions(8-node elements)

Lx=Lz=pi/3. , Ly=pi/4. (pi=3.1415926535)
number of nodes in x-direction = 12
" y-direction = 12
" z-direction = 12
hx=hz=pi/9. , hy=pi/12.

approx-eigenvalue	modes	actual-eigenvalue
2.37084	-------	--------
9.83625	-------	--------
11.72376	-------	--------
11.72376		
19.69684	(1,0,1)	18.00000
19.69684		
27.35672	(0,1,1)	25.00000
27.35672		
27.35672	(1,1,0)	
27.35672		
30.68483	-------	--------
34.39606	-------	--------
34.39606		
35.81914	-------	--------
36.22030	-------	--------
58.39643	-------	--------
59.09051	(1,0,2)	45.00000
59.09051		
59.09051	(2,0,1)	
59.09051		
66.12458	-------	--------
66.12458		
66.75040	(0,1,2)	52.00000
66.75040		
66.75040	(2,1,0)	
66.75040		
75.34928	-------	--------
75.34928		
91.37144	-------	--------
97.38992	(0,2,1)	73.00000
97.38992		
97.38992	(1,2,0)	
97.38992		
98.38694	-------	--------
98.48419	(2,0,2)	72.00000
98.48419		

Table 2. Similar results to Table 1 but with a different cavity shape.

CURL-CURL-bilinear elements(4-node elements)

Lx=Lz=pi/3. , Ly=pi/4. (pi=3.1415926535)
number of nodes in x-direction = 11
" y-direction = 11
" z-direction = 11
hx=hz=pi/9. , hy=pi/12.

approx-eigenvalue	modes	actual-eigenvalue
0.00000		
0.00000		
0.00000		
0.00000		
0.00000		
0.00000		
0.00000		
0.00000		
19.69684	(1,0,1)	18.00000
27.35672	(0,1,1)	25.00000
27.35672	(1,1,0)	
37.20514	(1,1,1)	34.00000
37.20514		
59.09052	(1,0,2)	45.00000
59.09052	(2,0,1)	
66.75040	(0,1,2)	52.00000
66.75040	(0,2,1)	
76.59882	(1,1,2)	61.00000
76.59882		
76.59882	(2,1,1)	
76.59882		
97.38992	(0,2,1)	73.00000
97.38992	(1,2,0)	
98.48419	(2,0,2)	72.00000
107.23834	(1,2,1)	82.00000
107.23834		
115.99249	(2,1,2)	88.00000
115.99249		

Table 3. The eigenvalues of the vector wave equation obtained by using constant-bilinear approximation functions. The zero modes may be ignored. Notice that all actual physical, eigenvalues are correctly approximated by this procedure although errors in the values are large for the higher-order modes.

CURL-CURL-bilinear functions(4-node elements)

Lx=Ly=Lz=pi/3. (pi=3.1415926535)
number of nodes in x-direction = 11
" y-direction = 11
" z-direction = 11
hx=hy=hz=pi/9.

approx-eigenvalue	modes	actual-eigenvalue
0.00000		
0.00000		
0.00000		
0.00000		
0.00000		
0.00000		
0.00000		
0.00000		
19.69684	(0,1,1)	18.00000
19.69684	(1,0,1)	
19.69684	(1,1,0)	
29.54526	(1,1,1)	27.00000
29.54526		
59.09052	(0,1,2)	45.00000
59.09052	(0,2,1)	
59.09052	(1,0,2)	
59.09052	(2,0,1)	
59.09052	(1,2,0)	
59.09052	(2,1,0)	
68.93893	(1,1,2)	54.00000
68.93893		
68.93893	(1,2,1)	
68.93893		
68.93893	(2,1,1)	
68.93893		
98.48419	(0,2,2)	72.00000
98.48419	(2,0,2)	
98.48419	(2,2,0)	
108.33261	(1,2,2)	81.00000
108.33261		
108.33261	(2,1,2)	
108.33261		
108.33261	(2,2,1)	
108.33261		

Table 4. Similar results to Table 1 but with a different cavity shape.

CURL-CURL-linear-biquadratic(18-node elements)

Lx=Ly=Lz=pi/3. (pi=3.1415926535)
number of nodes in x-direction = 18
" y-direction = 18
" z-direction = 18
hx=hy=hz=pi/9.

approx-eigenvalue	modes	actual-eigenvalue
0.00000	---	---
0.00000		
0.00000		
0.00000		
0.00000		
0.00000		
0.00000		
0.00000		
0.00000		
0.00000		
0.00000		
0.00000		
0.00000		
0.00000		
0.00000		
0.00000		
0.00000		
0.00000		
0.00000		
0.00000		
0.00000		
0.00000		
0.00000		
0.00000		
18.02846	(0,1,1)	18.00000
18.02846	(1,0,1)	
18.02846	(1,1,0)	
27.02822	(1,1,1)	27.00000
27.02822		
45.80279	(0,1,2)	45.00000
45.80279	(0,2,1)	
45.80279	(1,0,2)	
45.80279	(2,0,1)	
45.80279	(1,2,0)	
45.80279	(2,1,0)	
54.06912	(1,1,2)	54.00000
54.06912		
54.06912	(1,2,1)	
54.78579		
54.78579	(2,1,1)	
54.78579		
73.57712	(0,2,2)	72.00000
73.57712	(2,0,2)	
73.57712	(2,2,0)	
78.67638	---	---
78.67638		

CURL-CURL-linear-biquadratic(18-node elements)

Lx=pi/2. , Ly=pi/3. , Lz=pi/4. (pi=3.1415926535)
number of nodes in x-direction = 18
" y-direction = 18
" z-direction = 18
hx=pi/6. , hy=pi/9. , hz=pi/16.

approx-eigenvalue	modes	actual-eigenvalue
0.00000	-------	--------
0.00000		
0.00000		
0.00000		
0.00000		
0.00000		
0.00000		
0.00000		
0.00000		
0.00000		
0.00000		
0.00000		
0.00000		
0.00000		
0.00000		
0.00000		
0.00000		
0.00000		
0.00000		
0.00000		
0.00000		
0.00000		
0.00000		
0.00000		
0.00000		
13.02056	(0,1,1)	13.00000
20.03163	(1,0,1)	20.00000
25.03953	(0,1,1)	25.00000
25.36470	(2,1,0)	
29.02859	(1,1,1)	29.00000
29.03043		
32.37577	(2,0,1)	32.00000
40.00222	-------	--------
40.79489	(1,2,0)	40.00000
41.36763	(2,1,1)	41.00000
45.48986	(3,1,0)	45.00000
52.50093	(0,2,1)	52.00000
52.81386	(2,2,0)	
53.13903	(3,0,1)	
55.97965	------	--------
56.78009	(1,2,1)	56.00000
61.47941	(3,1,1)	61.00000
61.49460	-------	--------
62.74550	-------	--------
68.25079	(2,2,1)	68.00000
69.40821	(1,0,2)	
73.26419	(3,2,0)	72.00000

LAPLACIAN-trilinear functions(8-node elements)

Lx=Ly=Lz=pi/3. (pi=3.1415926535)
number of nodes in x-direction = 4
" y-direction = 4
" z-direction = 4
hx=hy=hz=pi/9.

approx-eigenvalue		modes	actual-eigenvalue
(19.69684,0.0000000)	2	(0,1,1)	(18.00000,0.0000000)
(29.54527,0.0000000)	3	(1,1,1)	(27.00000,0.0000000)
(59.09052,0.0000000)	5	(0,1,2)	(45.00000,0.0000000)
(59.09051,0.0000000)		(0,2,1)	
(68.93894,0.0000000)	6	(1,1,2)	(54.00000,0.0000000)
(68.93893,0.0000000)		(1,2,1)	
(68.93893,0.0000000)		(2,1,1)	
(98.48419,0.0000000)	8	(0,2,2)	(72.00000,0.0000000)
(108.3326,0.0000000)	9	(1,2,2)	(81.00000,0.0000000)
(108.3326,0.0000000)		(2,1,2)	
(108.3326,0.0000000)		(2,2,1)	

Table 7. Eigenvalues of the vector Helmholtz equation (Laplacian operator) obtained by using trilinear approximation functions. Note that all actual physical eigenvalues are correctly approximated by this procedure.

LAPLACIAN-trilinear functions(8-node elements)

Lx=Lz=pi/3. , Ly=pi/4. (pi=3.1415926535)
number of nodes in x-direction = 4
" y-direction = 4
" z-direction = 4
hx=hz=pi/9. , hy=pi/12.

approx-eigenvalue	modes	actual-eigenvalue
(27.35672,0.0000000)	(0,1,1)	(25.00000,0.0000000)
(37.20514,0.0000000)	(1,1,1)	(34.00000,0.0000000)
(66.75041,0.0000000)	(0,1,2)	(52.00000,0.0000000)
(76.59882,0.0000000)	(1,1,2)	(61.00000,0.0000000)
(76.59882,0.0000000)	(2,1,1)	
(97.38994,0.0000000)	(0,2,1)	(73.00000,0.0000000)
(107.2384,0.0000000)	(1,2,1)	(82.00000,0.0000000)
(115.9925,0.0000000)	(2,1,2)	(88.00000,0.0000000)
(125.8409,0.0000000)	(0,1,3)	(97.00000,0.0000000)
(136.7836,0.0000000)	(0,2,2)	(100.0000,0.0000000)
(146.6320,0.0000000)	(2,2,1)	(109.0000,0.0000000)
(146.6320,0.0000000)	(1,2,2)	

Table 8. Similar results to Table 7 but with a different cavity shape.

LAPLACIAN-bilinear functions(4-node elements)

Lx=Ly=Lz=pi/3. (pi=3.1415926535)
number of nodes in x-direction = 4
" y-direction = 4
" z-direction = 3
hx=hy=hz=pi/9.

approx-eigenvalue	modes	actual-eigenvalue
(19.69684,0.0000000)	(0,1,1)	(18.00000,0.0000000)
(19.69684,0.0000000)		
(19.69684,0.0000000)		
(59.09051,0.0000000)	(0,1,2)	(45.00000,0.0000000)
(59.09051,0.0000000)		
(59.09051,0.0000000)		
(59.09051,0.0000000)	(0,2,1)	(45.00000,0.0000000)
(59.09051,0.0000000)		
(59.09051,0.0000000)		
(98.48419,0.0000000)	(0,2,2)	(72.00000,0.0000000)
(98.48419,0.0000000)		
(98.48419,0.0000000)		

Table 9. Eigenvalues of the vector Helmholtz equation obtained by using constant-bilinear approximation functions. Notice that only the 0-mode eigenvalues are produced.

LAPLACIAN-bilinear functions(4-node elements)

Lx=Lz=pi/3. , Ly=pi/4. (pi=3.1415926535)
number of nodes in x-direction = 4
" y-direction = 4
" z-direction = 3
hx=hz=pi/9. , hy=pi/12.

approx-eigenvalue	modes	actual-eigenvalue
(27.35672,0.0000000)	(0,1,1)	(25.00000,0.0000000)
(27.35672,0.0000000)		
(27.35672,0.0000000)		
(66.75039,0.0000000)	(0,1,2)	(52.00000,0.0000000)
(66.75039,0.0000000)		
(66.75039,0.0000000)		
(97.38992,0.0000000)	(0,2,1)	(73.00000,0.0000000)
(97.38992,0.0000000)		
(97.38992,0.0000000)		
(136.7836,0.0000000)	(0,2,2)	(100.0000,0.0000000)
(136.7836,0.0000000)		
(136.7836,0.0000000)		

Table 10. Similar results to Table 9 but with a different cavity shape.

LAPLACIAN-bilinear functions(4-node elements)

Lx=Lz=pi/3. , Ly=pi/4. (pi=3.1415926535)
number of nodes in x-direction = 5
" y-direction = 7
" z-direction = 6
hx=hz=pi/15. , hy=pi/24.

approx-eigenvalue	modes	actual-eigenvalue
(25.66859,0.0000000)	(0,1,1)	(25.00000,0.0000000)
(25.66859,0.0000000)		
(25.66859,0.0000000)		
(25.66859,0.0000000)		
(25.66859,0.0000000)		
(57.30186,0.0000000)	(0,1,2)	(52.00000,0.0000000)
(57.30186,0.0000000)		
(57.30186,0.0000000)		
(57.30186,0.0000000)		
(57.30186,0.0000000)		
(79.33304,0.0000000)	(0,2,1)	(73.00000,0.0000000)
(79.33304,0.0000000)		
(79.33304,0.0000000)		
(79.33304,0.0000000)		
(79.33304,0.0000000)		
(110.9663,0.0000000)	(0,2,2)	(100.0000,0.0000000)
(110.9663,0.0000000)		
(110.9663,0.0000000)		
(110.9663,0.0000000)		
(110.9663,0.0000000)		

Table 11. Similar results to Table 10 but with a finer discretization.

LAPLACIAN-linear-biquadratic functions(18-node elements)

Lx=Ly=Lz=pi/3. (pi=3.1415926535)
number of nodes in x-direction = 4
" y-direction = 7
" z-direction = 7
hx=hy=hz=pi/9.

approx-eigenvalue	modes	actual-eigenvalue
18.02849	(0,1,1)	18.00000
27.87692	(1,1,1)	27.00000
45.80283	(0,1,2)	45.00000
45.80284	(0,2,1)	
55.65121	(1,1,2)	54.00000
55.65127	(1,2,1)	
67.27062	-- ? --	
73.57719	(0,2,2)	72.00000
83.42559	(1,2,2)	81.00000
91.08446	(0,3,1)	90.00000
91.08447	(0,1,3)	
95.04494	-- ? --	
95.04499	-- ? --	

Table 12. Eigenvalues of the vector Helmholtz equation obtained by using linear-biquadratic approximation functions. In this case, all eigenvalues are approximated, but the 0-mode eigenvalues are far more accurate than the non 0-mode eigenvalues.

LAPLACIAN-linear-biquadratic(18-node elements)

Lx=pi/2. , Ly=pi/3. , Lz=pi/4. (pi=3.1415926535)
number of nodes in x-direction = 4
" y-direction = 7
" z-direction = 7
hx=pi/6. , hy=pi/9. , hz=pi/12.

approx-eigenvalue	modes	actual-eigenvalue
25.03956	(0,1,1)	25.00000
29.41665	(1,1,1)	29.00000
46.92494	(2,1,1)	41.00000
52.81389	(0,2,1)	52.00000
57.19098	(1,2,1)	56.00000
68.81034	(0,1,2)	68.00000
74.41617	(1,1,2)	72.00000
74.69928	(3,1,1)	61.00000
78.79325	(2,2,1)	68.00000
96.30156	(2,1,2)	84.00000
96.58467	(3,2,1)	88.00000
98.09551	(0,3,1)	97.00000
102.1905	(0,2,2)	100.0000

Table 13. Similar results to Table 12 but with a different cavity shape.

MISSION
of
Rome Air Development Center

RADC plans and executes research, development, test and selected acquisition programs in support of Command, Control Communications and Intelligence (C^3I) activities. Technical and engineering support within areas of technical competence is provided to ESD Program Offices (POs) and other ESD elements. The principal technical mission areas are communications, electromagnetic guidance and control, surveillance of ground and aerospace objects, intelligence data collection and handling, information system technology, solid state sciences, electromagnetics and electronic reliability, maintainability and compatibility.

Printed by
United States Air Force
Hanscom AFB, Mass. 01731

END

FILMED

4-86

DTIC